NATIONAL ADVISORY COMMITTEE FOR AERONAUTICS

WARTIME REPORT

ORIGINALLY ISSUED

August 1945 as

Advance Restricted Report L5G18

STRESSES NEAR THE JUNCTURE OF A CLOSED AND AN OPEN TORSION BOX AS INFLUENCED BY BULKHEAD FLEXIBILITY

By Paul Kuhn and Harold G. Brilmyer

Langley Memorial Aeronautical Laboratory
Langley Field, Va.

NACA

WASHINGTON

L - 2

NATIONAL ADVISORY COMMITTEE FOR AERONAUTICS

ADVANCE RESTRICTED REPORT

STRESSES NEAR THE JUNCTURE OF A CLOSED AND AN OPEN TORSION BOX AS INFLUENCED BY BULKHEAD FLEXIBILITY

By Paul Kuhn and Harold G. Brilmyer

SUMMARY

A structure consisting of an open box joined to a closed box was subjected to torsional loading. Stress surveys were made first with a stiff bulkhead and then with a flexible one at the discontinuity. The results were compared with stresses calculated by a previously published theory, extended in this paper to take into account the flexibility of the bulkhead at the discontinuity. It was found that the stress distribution is not sensitive to bulkhead stiffness when this stiffness is large, and the experimental stresses agreed fairly well with the calculated stresses under such test conditions. When the bulkhead stiffness was small, however, the calculations became sensitive to errors in estimating this stiffness; such errors may be caused, for instance, by neglecting the effect of rivet deformation. The method of calculation is shown in detail for one case.

INTRODUCTION

The theory of stress distribution near discontinuities is fairly well developed for structural members of compact cross section. It is only slightly developed for members of the thin-walled stiffened-shell type, however, because even the basic theories for such members are of relatively recent origin. The present paper discusses one of the discontinuity problems frequently arising in the analysis of the smaller types of military airplane, namely, the problem of an open box joined to a closed box and subjected to torsion. The high speeds achieved by military airplanes dictate wing structures consisting of closed box-beams, but in the vicinity of the root it often

[redacted]

becomes necessary to employ an open box in order to permit retraction of the landing gear or insertion of gas tanks into the wing. The juncture between the closed and the open box presents problems in stress analysis that were included as special cases in a previous paper on the general theory of bending stresses due to torsion (reference 1). The theory presented in reference 1 assumes that the bulkheads are perfectly rigid; the error entailed by this assumption may become appreciable in the case under discussion here, because the bulkhead transferring torque from a closed box to an open one is heavily loaded. The theory was therefore extended slightly to take bulkhead flexibility into account, and this extension is presented in appendix A. Tests were made on a model structure, first with a very stiff bulkhead and then with a very flexible one. Comparisons of the experimental stresses with those calculated by the extended theory are shown. The calculations are given in detail for one case (appendix B).

SYMBOLS

a	length of bay (in combination bay, length of closed box)
b	width of box
c	depth of box
d	length of open box (in combination bay)
t	thickness of sheet
p, q, w	coefficients defined in reference 1
A	effective cross-sectional area of spar cap (corner flange)
E	Young's modulus of elasticity
G	shear modulus of elasticity
T	torque
X	force in spar cap at analysis station

σ	stress in spar cap
τ	shear stress in sheet

Subscripts:

b	pertaining to horizontal walls
c	pertaining to vertical walls
e	effective
B	pertaining to bulkhead at discontinuity (juncture between open and closed box)
D	located at discontinuity station

GENERAL DISCUSSION OF THE PROBLEM

If a torque T is applied at the tip of a two-spar wing structure, the transverse force acting on each spar is T/b (fig. 1) and the running shear in the spar web is

$$\tau t = \frac{T}{bc} \tag{1}$$

The bending moment in each spar is zero at the tip and increases linearly toward the root.

A box structure absorbs torque by shear in the walls (fig. 2); the running shear is constant in all four walls and is given by the basic formula for a thin-walled torsion box

$$\tau t = \frac{T}{2bc} \tag{2}$$

No bending moments exist in such a torque box.

Airplane wings frequently have full-width cut-outs with no cover or with covers of negligible effectiveness in carrying stress. The region of the cut-out is therefore an open box that acts like a two-spar structure under torsional loads (reference 2). The entire structure is then a statically indeterminate combination of a box and a two-spar structure (fig. 3). The presence of the box structure constrains the spars to deform as shown schematically in figure 4(a). The constraint is exerted by means of forces X_D acting on the spar flanges and constituting restraining moments as shown in figure 4(b). If the box were perfectly rigid, each spar would deform in such a manner that the tangent to its elastic curve at the discontinuity station D would remain parallel to the corresponding tangent at the root station R. With spars of constant section, there would be a point of inflection halfway between the discontinuity station and the root. The restraining moment at the discontinuity would be equal and opposite to the bending moment at the root, and the moments could be computed very easily because the transverse shear force on each spar is again T/b. In an actual box with finite stiffness, the restraining moment would be less than the moment at the root, and the point of inflection in the spar would be somewhere between the discontinuity station and the halfway point.

In the two-spar region of the structure, the entire torque T is carried by the transverse forces in the shear webs. In the box region, only one-half of the torque would be carried by the shear webs if the box were a free box, as can be deduced immediately from a comparison of formulas (1) and (2). At the juncture between the two regions, therefore, some torque must be transferred from the shear webs to the covers by the bulkhead. It might be surmised that this transfer would be effected in such a manner that the torque carried by the shear webs remains between the two values of T/2 and T. Calculations show, however, that the bulkhead actually "overdoes its job." The running shear in the cover sheets is increased beyond the value of T/2bc given by the simple torsion-box formula (2), and the shear in the webs is correspondingly below the value of T/2bc instead of being between this value and the value of T/bc that it has in the two-spar region. The amount of "overshooting" may be appreciable when the bulkhead is stiff. With increasing distance from the discontinuity the stress condition defined by formula (2) is approached, provided that the box has intermediate bulkheads. A qualitative picture of the shear-stress distribution is given by the solid lines in figure 5(a).

A general theory for calculating the stresses in combination structures of the type discussed here is given in reference 1. This theory is based on the assumption that all bulkheads are rigid in their respective planes. The calculations presented by Ebner (reference 3) indicate that this assumption is sufficiently accurate for practical purposes if adjacent bays are not too dissimilar. At a marked discontinuity such as the transition from an open box to a closed box, however, it may be advisable to take into account the finite stiffness of the bulkhead. The theory of reference 1 can be extended quite easily to cover this case, and the result of this extension is given in appendix A.

A qualitative picture of the stress changes brought about by increasing the flexibility of the bulkhead may be had by comparing the short-dash lines with the solid lines in figure 5. In the cover sheet, the shear stresses are decreased in the inboard bay and increased in the outboard bay as indicated in figure 5(a). Opposite changes necessarily take place in the shear webs to maintain equilibrium with the external torque. Figure 5(b) indicates that increased flexibility of the bulkhead results in increased bending moments at the root, decreased bending moments at the discontinuity, and a lower rate of decrease of the bending moments toward the tip.

The theory of reference 1 assumes that the walls of the box carry only shear and that longitudinal forces are absorbed entirely by concentrated corner flanges or spar caps. Actually, some of the longitudinal force is absorbed by the walls (including stringers if they exist). It is necessary, therefore, to add to the area of the actual spar caps some area equivalent to the walls insofar as absorption of longitudinal forces is concerned. It may also be advisable to make some allowance for the shear stresses incident to the diffusion of part of the flange force into the walls. These details are discussed more fully in the section "Theoretical Calculations" and in appendix B.

TEST SPECIMEN AND TEST PROCEDURE

The test specimen for the first series of tests (fig. 6) was a 24S-T aluminum-alloy box structure. The specimen was symmetrical about the plane of the root bulkhead. Because the structure as well as the loading was symmetrical about this plane, the spars could be considered to be perfectly fixed at the root bulkhead. The numbering of the bays is needed only for the analysis (appendix B) and is in accordance with the rules of reference 1. The bulkhead between bay 1 and bay 2, which is not shown in detail in figure 6, was of $\frac{3}{64}$-inch-thick steel.

For the first series of tests, the bulkhead at the discontinuity was made of $\frac{1}{8}$-inch-thick steel as shown on the main drawing of the test structure in figure 6. For the second series of tests, this stiff bulkhead was replaced by a flexible one made of 0.016-inch-thick aluminum-alloy sheet with vertical stiffeners spaced 5 inches apart. The cross section of this bulkhead is shown in the left upper corner of figure 6. For the third series of tests, the bulkhead was as shown in the right lower corner of figure 6. The bulkhead itself was the same one that was used in the second series of tests, but the steel cap angle on top was removed. The web of the flexible bulkhead was in a state of diagonal tension under the test loads.

For convenience, the three different bulkheads will be referred to as stiff bulkhead, flexible bulkhead with stiff cap-strip, and flexible bulkhead with flexible cap-strip, respectively. It should be noted that the so-called flexible cap-strip was theoretically not sufficiently flexible to cause nonuniform diagonal tension, but it did permit some local deformations in the corners of the bulkhead because, unlike the steel cap angle, it was not attached to the spar caps.

Torques were applied to the two ends of the structure by means of cables and winches. The loads were measured by dynamometers accurate to about 1/2 percent. The strain measurements were made with Tuckerman strain gages. Two-inch gages were used except on the cover sheets in the sheet bays adjacent to the corner flanges, where one-inch gages were used. Readings were taken at zero and at four equally spaced loads. Load-strain plots were made, and the readings were rejected if it was not possible to draw a straight line through the four points taken under load or if such a straight line missed the origin by more than 200 psi. The strains were converted to stresses by use of the values of $E = 10.6 \times 10^3$ ksi and $G = 4.0 \times 10^3$ ksi recommended in reference 4. The shear stresses in the sheet were determined from two sets of gage readings at 45° and 135°, respectively, to the axis of the structure.

THEORETICAL CALCULATIONS

The theoretical calculations were based on the method given in reference 1 for calculating bending stresses due to torsion. The slight modifications of the formulas that are necessary to take into account the flexibility of the bulkhead at the discontinuity are given in appendix A. The details of the calculation for the structure with the flexible bulkhead are given in appendix B. This calculation applies to the second and the third series of tests, because the only change made in the structure - removal of the steel cap angle on the bulkhead - theoretically did not increase the flexibility of the bulkhead. The calculations for the first series of tests differ from those shown only in the magnitude of the terms involving the bulkhead thickness.

The theory assumes that the walls carry only shear stresses, and that longitudinal stresses are absorbed by concentrated corner flanges or spar caps. The shear webs, the cover sheets, and the stringers must therefore be replaced by equivalent concentrated corner flanges for purposes of calculation. On the assumption that the chordwise distribution of the longitudinal stresses in a wall is linear, the equivalent area is one-sixth of the actual area of the wall (reference 2). This theoretical coefficient of 1/6 was considered sufficiently accurate to obtain the concentrated corner flanges equivalent to the shear webs.

For the cover sheets with their stringers, the theoretical coefficient 1/6 was considered not sufficiently accurate, chiefly because the length-width ratio was quite small. For the continuous bottom cover, including stringers, the equivalent area was estimated from stress measurements by two methods. The first method consisted in obtaining an experimental stress distribution across the cover at a station close to the discontinuity; the equivalent area was then computed from the integrated moment of these experimental stresses. The second method consisted in comparing the stress in the free spar cap with that in the spar cap attached to the cover at a number of stations in the open-box region. The first method gave a coefficient of about 1/15, and the second method gave an average coefficient of slightly more than 1/20. Because the second method was based on a much larger number of measurements, more weight was given to it than to the first method, and a round value of 1/20 was used.

At the intermediate bulkhead, the equivalent flange area of the discontinuous (top) cover might be assumed to equal that of the continuous cover; toward the two ends of the cover it drops to zero. The average equivalent area was therefore small and was neglected in the general calculations. The equivalent area of the discontinuous cover is needed, however, to calculate the local correction to the shear stress caused by the diffusion of part of the flange force into the cover near the discontinuity. (See appendix B.)

As a result of the assumptions made, the area A of each corner flange was constant from tip to root, but there were two different values of area - one for the flanges on the side of the continuous cover and one for the flanges on the side of the discontinuous cover. The individual flange areas were used for computing the stresses from the forces in the flanges, but the average of all the flange areas was used in the computation of the coefficients p, q, and w (appendix A). This procedure was necessary because the theory assumes all the flanges to be equal; it should entail no serious error because the two individual values did not differ greatly from each other, and trial calculations showed that large changes in the area A produced only small changes in the flange forces.

TEST RESULTS AND DISCUSSION

The spanwise distribution of the shear stresses in the shear webs is shown in figure 7. The measurements were taken in the first series of tests (stiff bulkhead); in the other two series, measurements on the shear webs were taken only in the box region. In the open box, the stresses were calculated by formula (1), by using for c the distance between centroids of the spar caps. The calculations for the region of the closed box were made as indicated in appendix B. As mentioned in the general discussion of the problem, the stress in the shear web just outboard of the discontinuity is much lower than would be calculated from the simple torsion formula (2) for a free-torsion box. In view of the small magnitude of the stresses, the agreement between calculated and experimental web shear stresses may be considered quite satisfactory.

The spar-cap stresses measured in the first and second series of tests are shown in figures 8 and 9, respectively. In the third series, measurements were taken only in the vicinity of the discontinuity; they agreed very closely with those taken in the second series and consequently are not shown. On the top spar caps, the stresses are influenced by lateral bending (reference 2) in the vicinity of the discontinuity and of the root. These lateral bending stresses account for the pronounced difference between the stresses in the median fiber and those in the outermost fiber just outboard of the discontinuity. The median fiber stresses were obtained by averaging the stresses on the outermost and the innermost fibers; theoretically, therefore, the effect of lateral bending was eliminated from the experimental stresses shown, but the investigation of lateral bending on these spar caps (reference 2) showed that the elimination may be incomplete because the caps do not act as integral units. In order to avoid confusion, no calculations for lateral bending are shown, but it might be well to point out that, with the flexible bulkhead, the stress in the innermost fiber (not shown) at the discontinuity is nearly equal to the stress in the median fiber at the root.

On the whole, the agreement between calculated and experimental spar-cap stresses may be considered satisfactory except on the top caps in the structure with the flexible bulkhead.

The shear stresses measured in the box part of the structure are shown in figures 10, 11, and 12. Running shears are shown rather than shear stresses because the scale is so small that the stresses in the shear web would be difficult to compare. As was to be expected, the stresses measured in the structure with the flexible bulkhead were almost identical, with the stiff cap-strip (fig. 11) or the flexible cap-strip (fig. 12). The only exceptions were the shear stresses in the corners of the discontinuous cover adjacent to the discontinuity. As indicated by the question marks beside the plotted points, however, these values are considered questionable in both series of tests because it is believed that they were probably falsified by buckling of the cover sheet, which was induced by the pull of the diagonal-tension field in the bulkhead. The check of static equilibrium between the shear force in the discontinuous cover and the shear force in the continuous cover for the station next to the bulkhead showed that the internal force in the discontinuous cover was about 10 percent too high for figure 11 as well as for figure 12. In figure 10, where no buckling took place, the same check showed an error of less than 0.2 percent. At all other stations in the three series of tests, the error in the static check was less than 1 percent except at the tip station in figure 12, where the error was 4 percent. When the points marked by question marks were discarded and the straight-line extrapolation from the two adjacent points was used, the error was reduced from 10 percent to about 5 percent. The high shear stresses in the corners are therefore probably spurious.

Direct evidence of falsification of measured stresses due to buckling was found on the web shears adjacent to the flexible bulkhead; these shears are omitted in figures 11 and 12 for this reason. The load-strain curves for these stations did not show a constant rate of change of strain with load, but a decreasing rate and finally a reversal. The effect was particularly pronounced on the two gage stations adjacent to those corners of the box where the tension diagonals of the bulkhead terminated.

A graphic presentation of the experimental stresses for all three test series is given in figure 13. In order to simplify the picture, faired curves are shown rather than individual measurements. The points marked with question marks in figures 11 and 12 were disregarded here. With the stiff bulkhead, the shears in the cover sheets of the bay adjacent to the discontinuity were considerably higher than the basic shear $T/2bc$; in the tip bay, the cover shears were lower but were still higher than the basic shear. With the flexible bulkhead, the shears in the cover of the bay adjacent to the discontinuity were reduced to an average value not much higher then the basic shear, but the shears in the tip bay were much higher than the basic shear.

A close comparison of experimental and calculated stresses in figures 10, 11, and 12 is somewhat difficult because the simple theory used gives uniform chordwise distributions (except on the discontinuous cover near the discontinuity), whereas the actual chordwise distributions tend to be variable. In order to overcome this difficulty, chordwise averages of the stresses were computed for each cover and for each station. Because these chordwise averages of the stresses differ from the internal forces only by a constant, the statements made above concerning the closeness of the static checks apply again. In view of these good static checks it was considered not worthwhile to give the individual stresses, and only the experimental averages for each bay were included in the final tabulation presented in table 1.

Two sets of calculated stresses are shown in table 1. The first set is based on a bulkhead shear stiffness $G_e t$ equal to 100 percent of the calculated stiffness; the second set is based on a stiffness equal to 70 percent of the calculated value. The second set was computed because a comparison of the ratios of experimental to calculated stresses for the first set indicated systematic differences of such a nature that the assumption of greater bulkhead flexibility would give better agreement. It will be noted that the improvement was insignificant for the stiff bulkhead but was appreciable for the flexible one; that is, the calculations were sensitive to bulkhead stiffness when the stiffness was small. Failure to achieve the full calculated stiffness may be attributed to rivet deformation and local deformation of the bulkhead in the corner. In all the tests, the agreement between experimental and calculated stresses was better for the bay adjacent to the discontinuity than for the tip bay. In the bay next to the discontinuity, agreement was good with the stiff bulkhead; with the flexible bulkhead good agreement apparently depended on a correct estimate of bulkhead stiffness.

The experimental shear stresses in the cover were changed by more than 20 percent by substituting a flexible bulkhead for the original stiff bulkhead. This large change indicates clearly that the stress analysis should take the bulkhead flexibility into account. Failure to achieve good agreement between theory and experiment in the tip bay can probably be attributed to the fact that the unaccountable effects mentioned - rivet deformation and local deformation of the bulkhead - were accentuated at the tip bulkhead where the torque was introduced in the form of concentrated forces.

CONCLUSIONS

The following conclusions were drawn, from the test data and the calculated results, concerning the stresses near the juncture of a closed with an open torsion box:

1. The measured stresses in the vicinity of the discontinuity agree satisfactorily with the calculated stresses provided the bulkhead at the discontinuity is stiff. If the bulkhead is flexible, close agreement can be achieved only if the effective shear stiffness of the bulkhead can be estimated correctly.

2. If the bulkhead stiffness is varied between somewhat wider limits than are likely to be found in actual construction, the shear stresses in the cover may change by more than 20 percent.

3. The chordwise distribution of the shear stresses is more variable than can be explained by the simple theory presented here.

Langley Memorial Aeronautical Laboratory
National Advisory Committee for Aeronautics
Langley Field, Va.

APPENDIX A

FORMULAS FOR COMBINATION BAYS WITH FLEXIBLE BULKHEADS

The shear stress in the bulkhead at the juncture between the open and the closed box part of a combination bay (reference 2) can be obtained by noting that the running shear acting on the bulkhead equals the running shear in the cover sheet terminating at the bulkhead, or

$$\tau_B t_B = \tau_b t_b$$

The value of τ_B obtained in this manner may be used to add terms representating the energy in the bulkhead in the derivations given in reference 1, with the following results:

(1) In the formulas for warping w_o^T or w_1^T (formulas (49), (50), (56), and (57) of reference 1), add

$$\frac{T}{16at_BG}$$

where t_B is the thickness of the bulkhead. For a combination bay of type II (see reference 1), which is the case discussed in this paper,

$$w_o^T = w^T + q\frac{Td}{bc} + \frac{T}{16at_BG}$$

(2) In the formulas for coefficients p and q (formulas (23) and (27) of reference 1), add

$$\frac{bc}{16a^2t_BG}$$

For instance

$$p = \frac{a}{3AE} + \frac{1}{8Ga}\left(\frac{b}{t_b} + \frac{c}{t_c}\right) + \frac{bc}{16a^2 t_B G}$$

The corrected form for p must be used in formula (40) of reference 1; similarly, the corrected forms for p and q must be used in formulas (49), (50), (56), and (57) for warping.

The corrected formulas apply only to bays having no intermediate ribs (assumption A of reference 1). For bays with closely spaced intermediate ribs (assumption B of reference 1), it would obviously be pointless to attempt to take into account the flexibility of the first bulkhead as long as the intermediate ribs are assumed to be rigid, as was done in reference 1. If the intermediate ribs are assumed to be flexible, all the formulas become more complicated, and it is believed that the gain in accuracy is too small to justify the added complications in most practical cases.

APPENDIX B

NUMERICAL ANALYSIS OF TEST STRUCTURE WITH FLEXIBLE BULKHEAD

Basic Data

As an example of the method of analysis, the stresses are analyzed near the juncture of a closed and an open torsion box like the test specimen discussed in the present paper. The case considered is that of the flexible bulkhead. Number subscripts 1 and 2 refer to bays or stations, numbered by the convention of reference 1. Bays are numbered as shown in figure 6. Station 1 is between bay 1 and bay 2; station 2 is the root. The basic data follow:

$a_1 = a_2 = 28$ in. $\quad b = 45$ in. $\quad c = 10$ in. $\quad d = 56$ in.

$t_b = 0.040$ in. $\quad t_c = 0.081$ in.

$T = 46.8$ in.-kips

$\frac{G}{E} = 0.377$ (from values of G and E used to convert strains to stresses)

Estimated effective shear modulus of bulkhead in diagonal tension $G_e = 0.62G$

Effective thickness of bulkhead $t_B = 0.62 \times 0.016 = 0.010$ in.

Cross-sectional area of actual corner flanges (two angles) = 0.470 sq in.

Equivalent flange area contributed by shear web $= \frac{1}{6} \times 0.81 = 0.135$ sq in.

Total effective area of top flanges = 0.470 + 0.135 = 0.605 sq in.

Equivalent flange area contributed by bottom cover $= \frac{1}{20} \times 3.25 = 0.163$ sq in.

Total effective area of bottom flanges
$= 0.470 + 0.135 + 0.163 = 0.768$ sq in.

Average effective flange area $= \frac{1}{2}(0.605 + 0.768)$
$\doteq 0.687$ sq in.

Calculation of Coefficients

The coefficients listed herein are calculated as indicated in appendix A by the formulas of reference 1. The formulas are used here in the modified form suggested in reference 1 for numerical work. The modification consists in multiplying through by G; the factor 1/G then disappears and the factor 1/E is replaced by G/E. The coefficients are

$$p_1 = \frac{aG}{3AE} + \frac{1}{8a}\left(\frac{b}{t_b} + \frac{c}{t_c}\right)$$

$$= \frac{28\times0.377}{3\times0.687} + \frac{1}{8\times28}\left(\frac{45}{0.040} + \frac{10}{0.081}\right)$$

$$= 5.14 + 5.57 = 10.71$$

$$q_1 = -\frac{aG}{6AE} + \frac{1}{8a}\left(\frac{b}{t_b} + \frac{c}{t_c}\right)$$

$$= -\frac{28\times0.377}{6\times0.687} + \frac{1}{8\times28}\left(\frac{45}{0.040} + \frac{10}{0.081}\right)$$

$$= -2.57 + 5.57 = 3.00$$

$$p_2 = \frac{aG}{3AE} + \frac{1}{8a}\left(\frac{b}{t_b} + \frac{c}{t_c}\right) + \frac{bc}{16a^2t_B}$$

$$= \frac{28\times0.377}{3\times0.687} + \frac{1}{8\times28}\left(\frac{45}{0.040} + \frac{10}{0.081}\right) + \frac{45\times10}{16\times(28)^2\times0.010}$$

$$= 5.14 + 5.57 + 3.59 = 14.30$$

$$q_2 = -\frac{aG}{6AE} + \frac{1}{8a}\left(\frac{b}{t_b} + \frac{c}{t_c}\right) + \frac{bc}{16a^2t_B}$$

$$= -2.57 + 5.57 + 3.59 = 6.59$$

$$p_2' = p_2 + \frac{dG}{AE}$$

$$= 14.30 + \frac{56\times0.377}{0.687}$$

$$= 14.30 + 30.82 = 45.12$$

$$w_1^T = \frac{T}{8bc}\left(\frac{b}{t_b} - \frac{c}{t_c}\right)$$

$$= \frac{T}{8\times45\times10}\left(\frac{45}{0.040} - \frac{10}{0.081}\right)$$

$$= 0.278T = 13.02$$

$$w_{2_0}^T = \frac{T}{8bc}\left(\frac{b}{t_b} - \frac{c}{t_c}\right) + q_2\frac{Td}{bc} + \frac{T}{16ct_B}$$

$$= 0.278T + 6.59\frac{T\times56}{45\times10} + \frac{T}{16\times28\times0.010}$$

$$= 0.278T + 0.820T + 0.223T$$

$$= 1.321T = 61.82$$

$$w_{2_1}^T = \frac{T}{8bc}\left(\frac{b}{t_b} - \frac{c}{t_c}\right) + p_2\frac{Td}{bc} + \frac{Td^2G}{2bcAE} + \frac{T}{16at_B}$$

$$= 0.278T + 14.30\frac{T\times56}{45\times10} + \frac{T\times(56)^2\times0.377}{2\times45\times10\times0.687} + 0.223T$$

$$= 0.278T + 1.779T + 1.918T + 0.223T$$

$$= 4.198T = 196.49$$

Calculation of X-Forces

Because the structure being analyzed has only two bays, the equations for the X-forces can be obtained by simply substituting $m = 2$ into equations (62) and (63) of reference 1:

$$-(p_1 + p_2)X_1 + q_2X_2 = -w_1{}^T + w_{2_o}{}^T$$

$$q_2X_1 - p_2'X_2 = -w_{2_i}{}^T$$

Substitution of the numerical values gives

$$-25.01X_1 + 6.59X_2 = -13.02 + 61.82 = 48.80$$

$$6.59X_1 - 45.12X_2 = -196.49$$

The solution of these equations is

$$X_1 = -0.837 \text{ kips} \qquad X_2 = 4.233 \text{ kips}$$

The X-force at the discontinuity is

$$X_D = X_2 - \frac{Td}{bc}$$

$$= 4.233 - 5.824 = -1.591 \text{ kips}$$

Calculation of Stresses

The stresses in the top flanges are

$$\sigma_1 = -\frac{0.837}{0.605} = -1.40 \text{ ksi}$$

$$\sigma_2 = \frac{4.233}{0.605} = 7.00 \text{ ksi}$$

$$\sigma_D = -\frac{1.591}{0.605} = -2.63 \text{ ksi}$$

The running shears in the cover sheet are obtained by the application of formulas (6) and (7) of reference 1 as

$$(\tau t)_1 = -\frac{X_1}{2a} + \frac{T}{2bc}$$

$$(\tau t)_2 = \frac{-X_D+X_1}{2a} + \frac{T}{2bc}$$

or numerically

$$(\tau t)_1 = -\frac{-0.837}{2\times 28} + \frac{46.8}{2\times 45\times 10}$$

$$= 0.0149 + 0.0520 = 0.0669 \text{ kips/in.}$$

$$(\tau t)_2 = \frac{1.591-0.837}{2\times 28} + 0.0520$$

$$= 0.0135 + 0.0520 = 0.0655 \text{ kips/in.}$$

The shear stress in the cover adjacent to the discontinuity is

$$\tau_2 = \frac{(\tau t)_2}{0.040} = \frac{0.0655}{0.040} = 1.637 \text{ ksi}$$

Correction to Shear Stress in Discontinuous Cover

At the inboard end of the discontinuous cover, the flange force X is introduced in concentrated form at the corner flange. The maximum shear stress in the adjacent sheet, caused by diffusing part of this force into the corner, may be calculated by formula (A-2) of reference 5. For large values of KL, this formula may be simplified to

$$\tau_{max} = \frac{XKA_L}{tA_T}$$

where the shear-lag parameter K is defined by

$$K = \sqrt{\frac{Gt}{Eb_S}\left(\frac{1}{A} + \frac{1}{A_L}\right)}$$

The symbols appearing in these two expressions apply directly to the properties of an idealized panel. The relations between idealized panels and actual flat panels have been established empirically (reference 6), but there is some doubt about the details of extending these relations to the case under consideration here, where the force X is applied to the corner flange of a box. For a wide shallow box, such as the test box, the following interpretation of the symbols is believed to be reasonable:

A effective cross-sectional area of corner flange including actual corner angles and equivalent area contributed by adjacent shear web

A_L equivalent area contributed to corner flange by discontinuous cover and its stringers

A_T sum of A and A_L

b_S substitute width $(b/4)$

t thickness of cover sheet

E Young's modulus of elasticity

G shear modulus of elasticity

Substitution of the numerical values then gives

$$K = \sqrt{\frac{0.377 \times 0.040}{11.25}\left(\frac{1}{0.605} + \frac{1}{0.163}\right)} = 0.102$$

and

$$\tau_{max} = \frac{1.591 \times 0.102 \times 0.163}{0.040 \times 0.768} = 0.865 \text{ ksi}$$

The shear associated with the diffusion of X_D into the cover and stringers must be distributed in such a way that it does not change the average transverse shear force. It was assumed that this shear is distributed parabolically over the width of the cover, and $0.67\tau_{max}$ was added to τ_2 to obtain the final shear stress in the corners while $0.33\tau_{max}$ was subtracted from τ_2 to obtain the shear stress at the center line of the cover sheet.

In view of the uncertainty in determining A_L, b_S, and the chordwise distribution of the shear correction, the method given must be considered as purely tentative.

REFERENCES

1. Kuhn, Paul: A Method of Calculating Bending Stresses Due to Torsion. NACA ARR, Dec. 1942.

2. Kuhn, Paul, Batdorf, S. B., and Brilmyer, Harold G.: Secondary Stresses in Open Box Beams Subjected to Torsion. NACA ARR No. L4I23, 1944.

3. Ebner, Hans: Torsional Stresses in Box Beams with Cross Sections Partially Restrained against Warping. NACA TM No. 744, 1934.

4. Templin, R. L., and Hartmann, E. C.: The Elastic Constants for Wrought Aluminum Alloys. NACA TN No. 966, 1945.

5. Kuhn, Paul: Approximate Stress Analysis of Multi-stringer Beams with Shear Deformation of the Flanges. NACA Rep. No. 636, 1938.

6. Kuhn, Paul, and Chiarito, Patrick T.: Shear Lag in Box Beams - Methods of Analysis and Experimental Investigations. NACA Rep. No. 739, 1942.

TABLE 1

COMPARISON OF EXPERIMENTAL AND CALCULATED

SHEAR STRESSES (PSI) IN CLOSED-BOX

PART OF STRUCTURE

Shear stress	Bay 1 (outboard bay)		[a]Bay 2 (inboard bay)	
	Cover	Shear web	Cover	Shear web
Stiff bulkhead				
Experimental	1587	538	1957	304
Calculated[b]	1425	580	2004	294
Experimental/calculated	1.113	0.928	0.974	1.034
Calculated[c]	1429	578	1998	297
Experimental/calculated	1.110	0.931	0.980	1.023
Flexible bulkhead, stiff cap-strip				
Experimental	1842	378	1477	538
Calculated[b]	1674	457	1637	476
Experimental/calculated	1.100	0.828	0.902	1.129
Calculated[c]	1756	417	1514	536
Experimental/calculated	1.049	0.907	0.974	1.002
Flexible bulkhead, flexible cap-strip				
Experimental	1927	388	1448	586
Calculated[b]	1674	457	1637	476
Experimental/calculated	1.150	0.849	0.885	1.230
Calculated[c]	1756	417	1514	536
Experimental/calculated	1.098	0.931	0.955	1.091

[a]Experimental stresses for bay 2 are average of 2 stations.
[b]Bulkhead stiffness considered 100 percent of calculated value.
[c]Bulkhead stiffness considered 70 percent of calculated value.

NATIONAL ADVISORY
COMMITTEE FOR AERONAUTICS

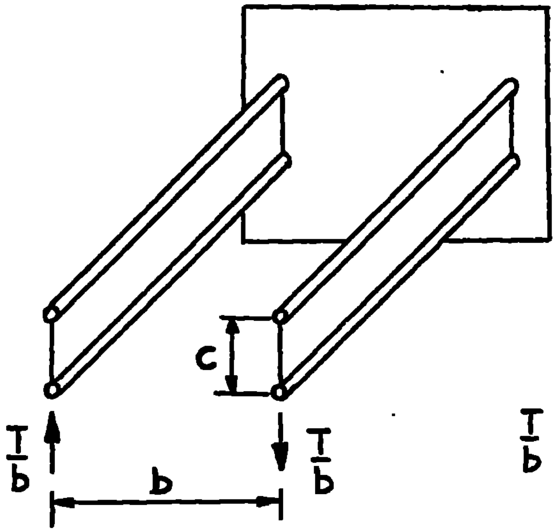

Figure 1.- Two-spar structure under torsion.

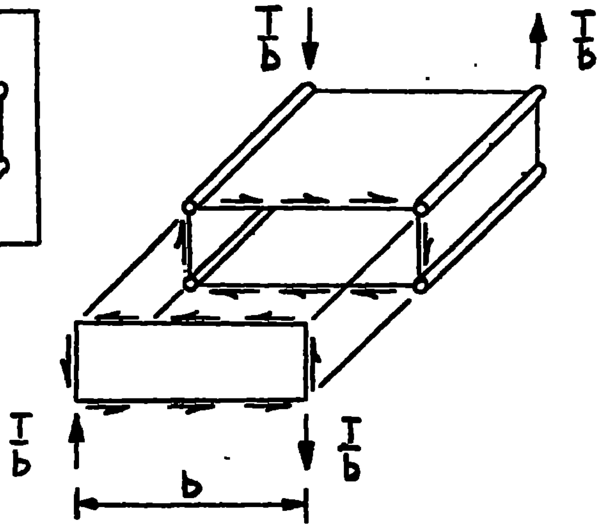

Figure 2.- Box under torsion.

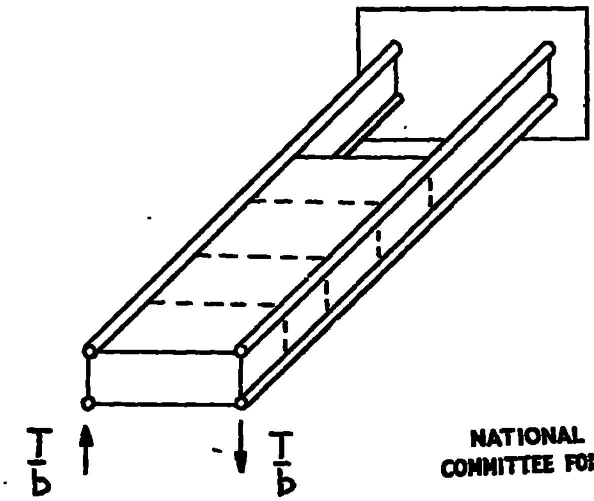

NATIONAL ADVISORY COMMITTEE FOR AERONAUTICS

Figure 3.- Combination box and two-spar structure under torsion.

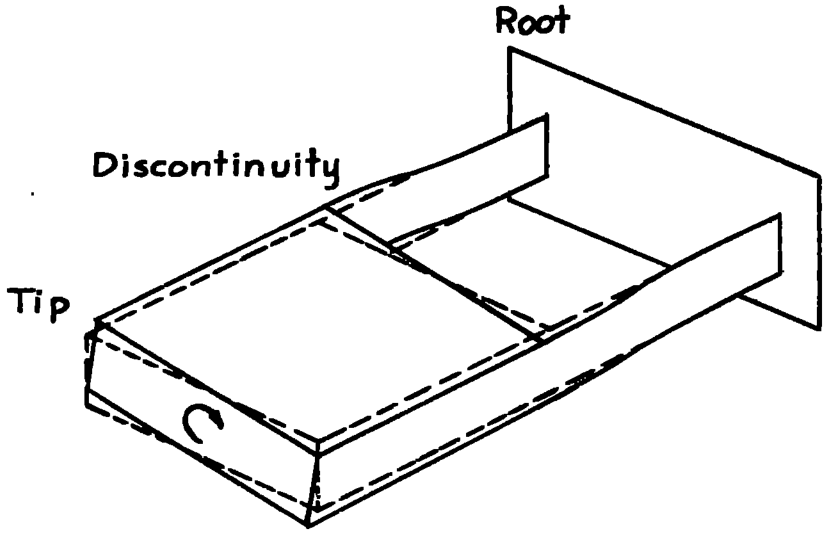

(a) Deformation of combination structure.

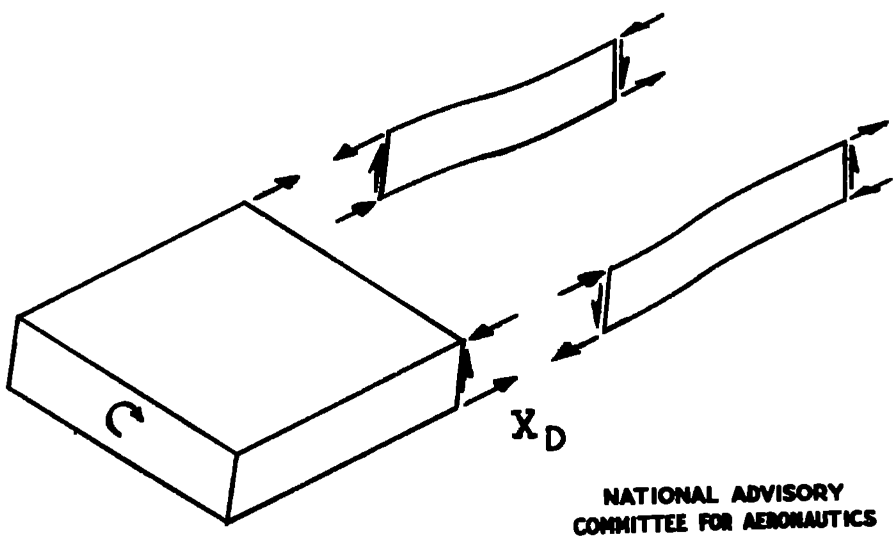

(b) Free-body diagrams of combination structure.

Figure 4.- Combination structure.

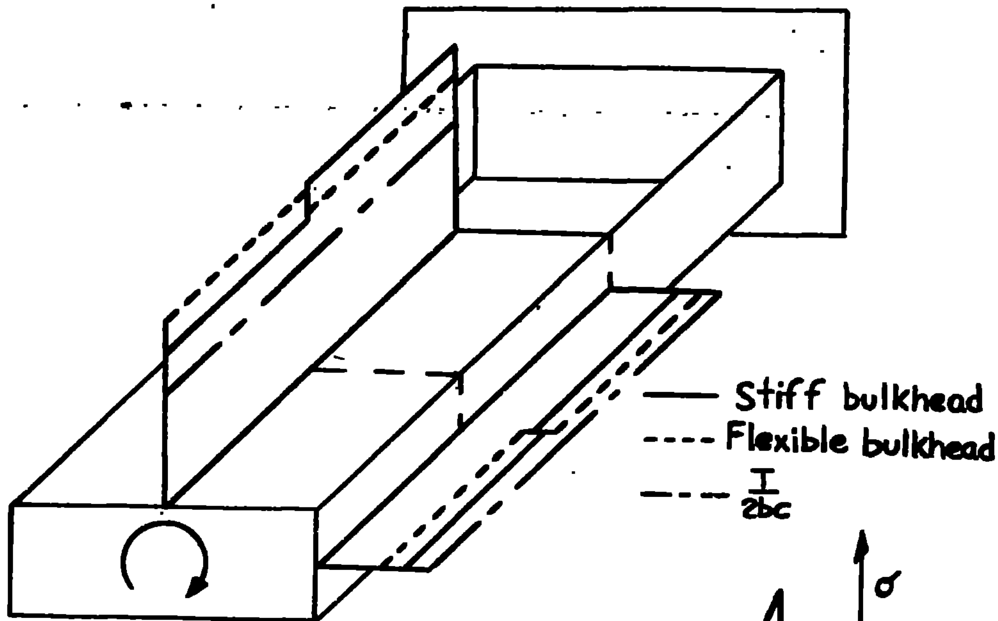

(a) Shear-stress distribution.

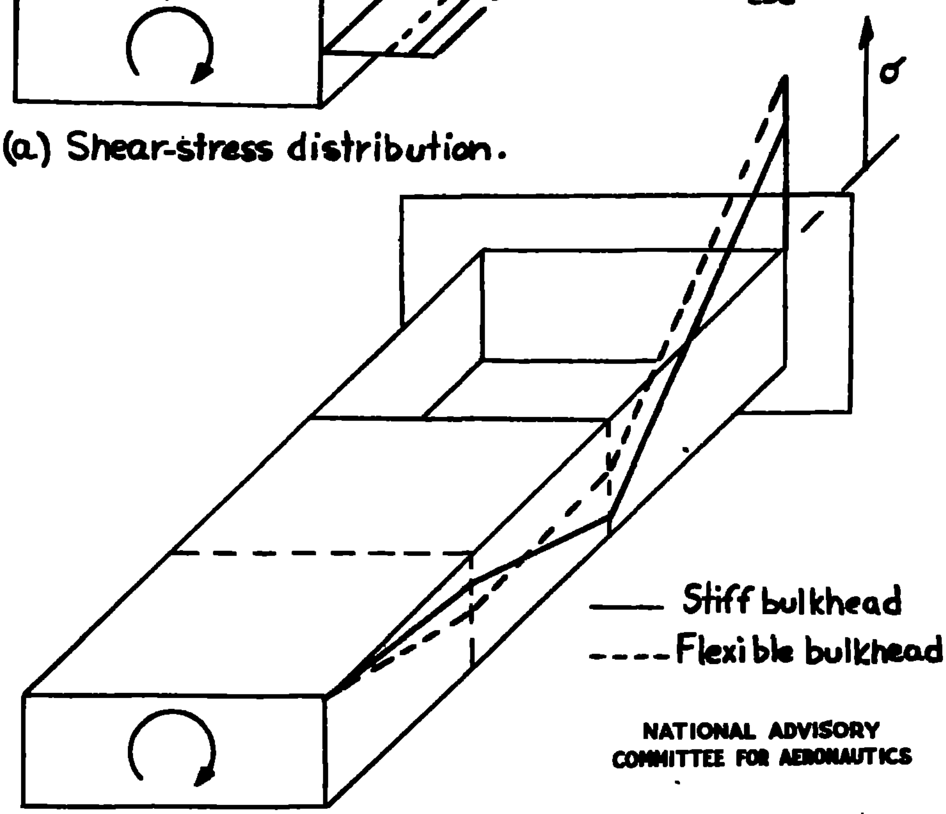

(b) Flange-stress distribution.

Figure 5.- Stress distribution in combination structure.

Fig. 6

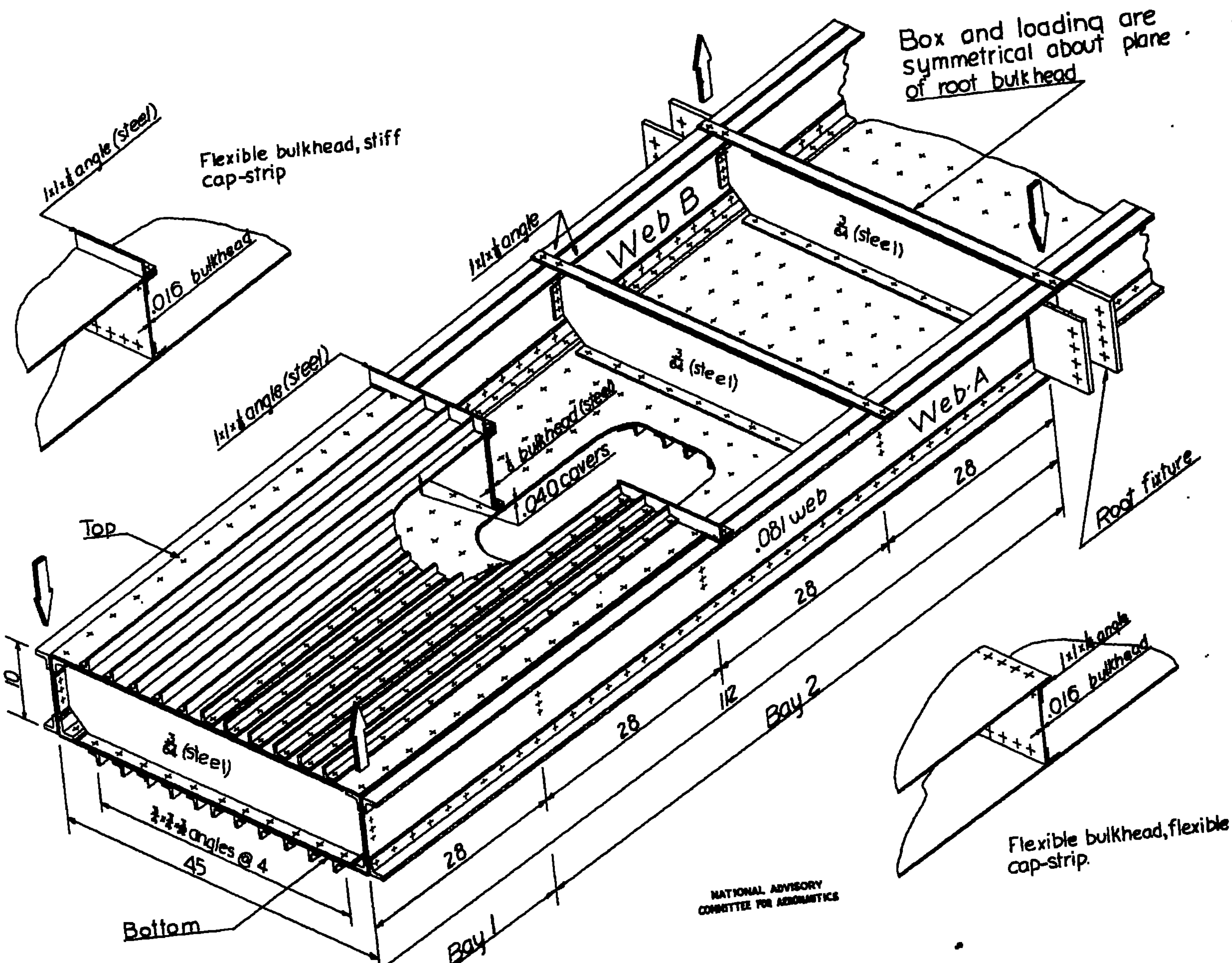

NATIONAL ADVISORY
COMMITTEE FOR AERONAUTICS

... aluminum alloy unless otherwise specified.

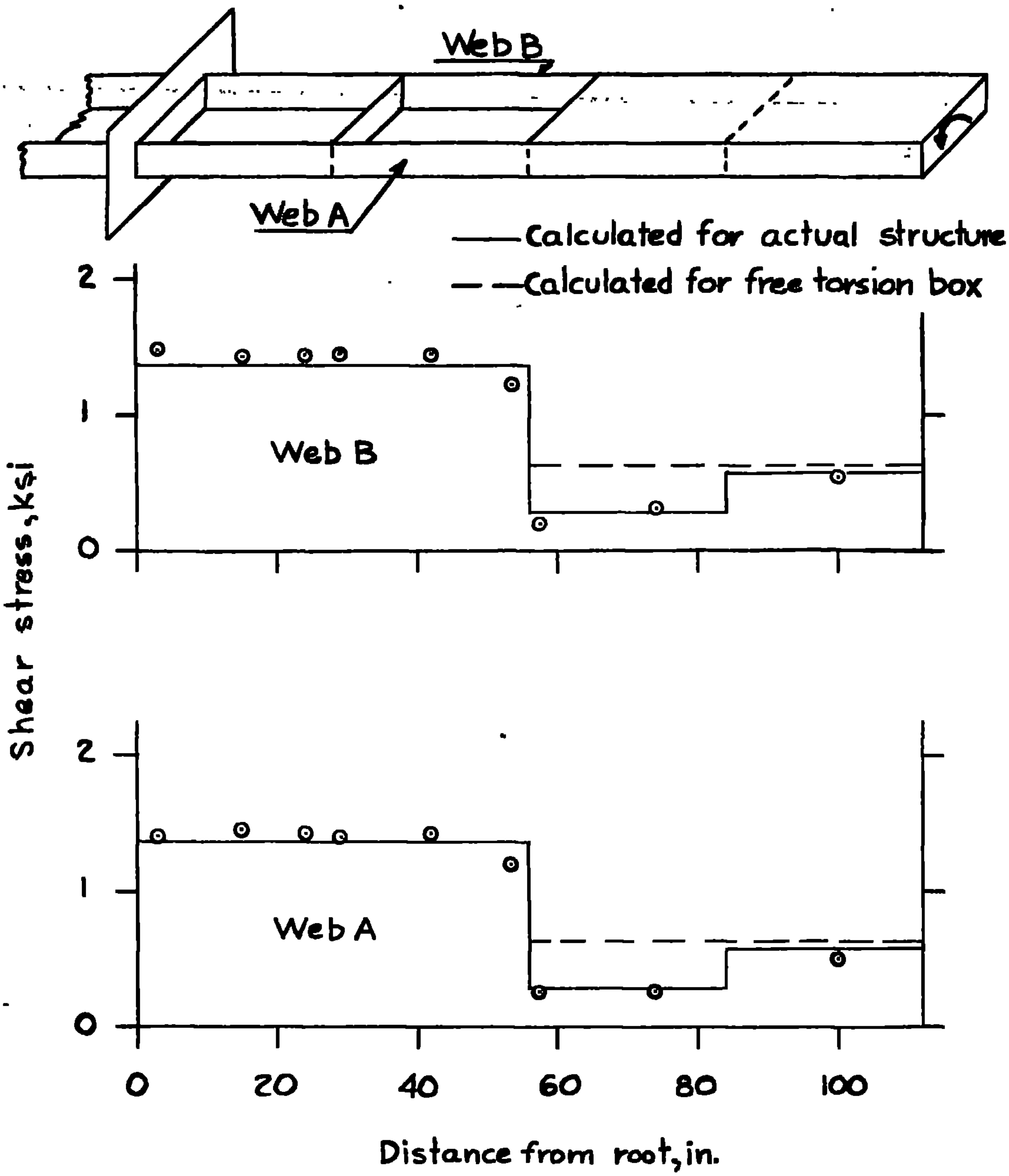

Figure 7.- Spanwise distribution of stresses in shear webs for box with stiff bulkhead at discontinuity.

NATIONAL ADVISORY
COMMITTEE FOR AERONAUTICS

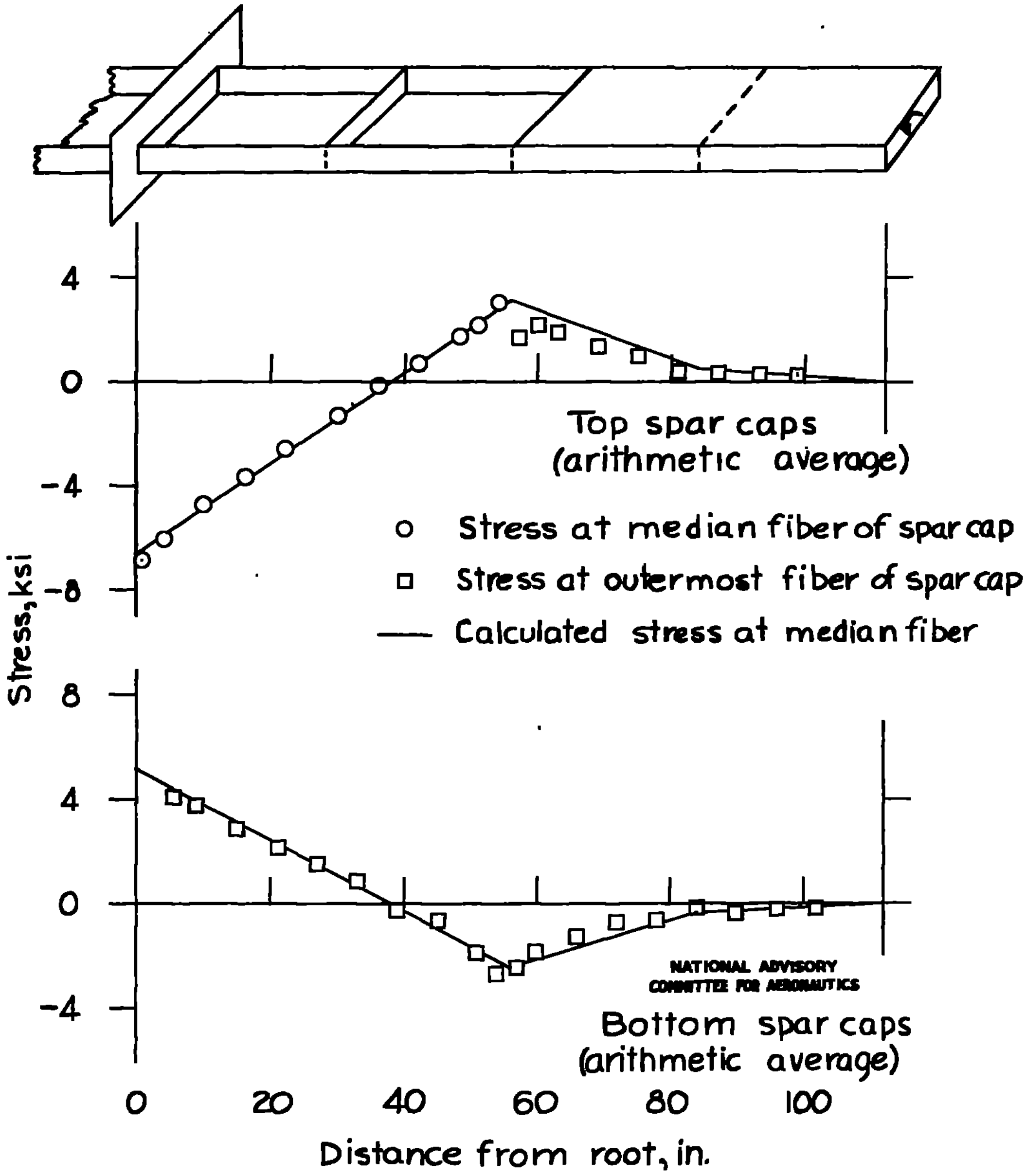

Figure 8.- Distribution of spar-cap stress in test structure with stiff bulkhead.

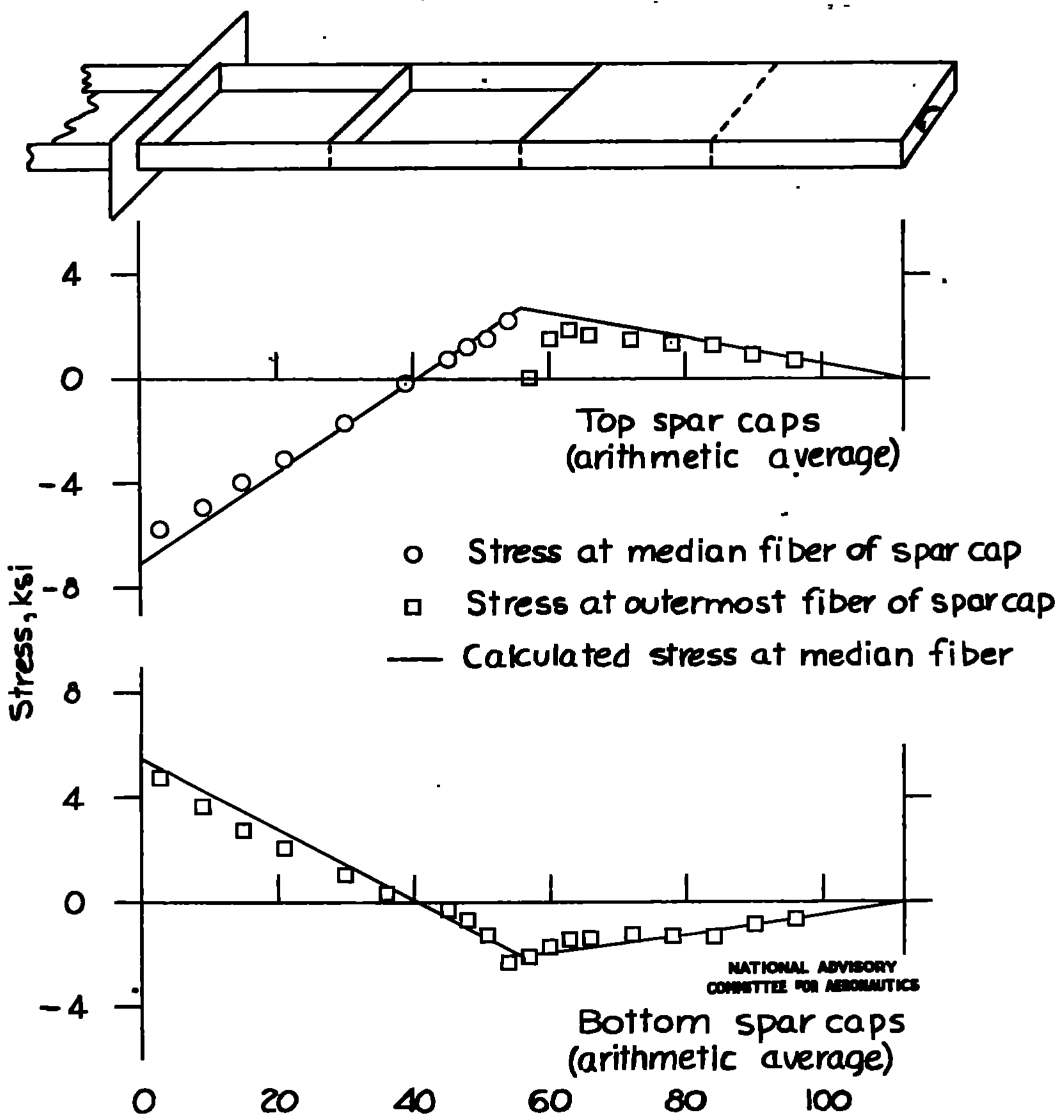

Figure 9.- Distribution of spar-cap stress in test structure with flexible bulkhead and stiff cap-strip.

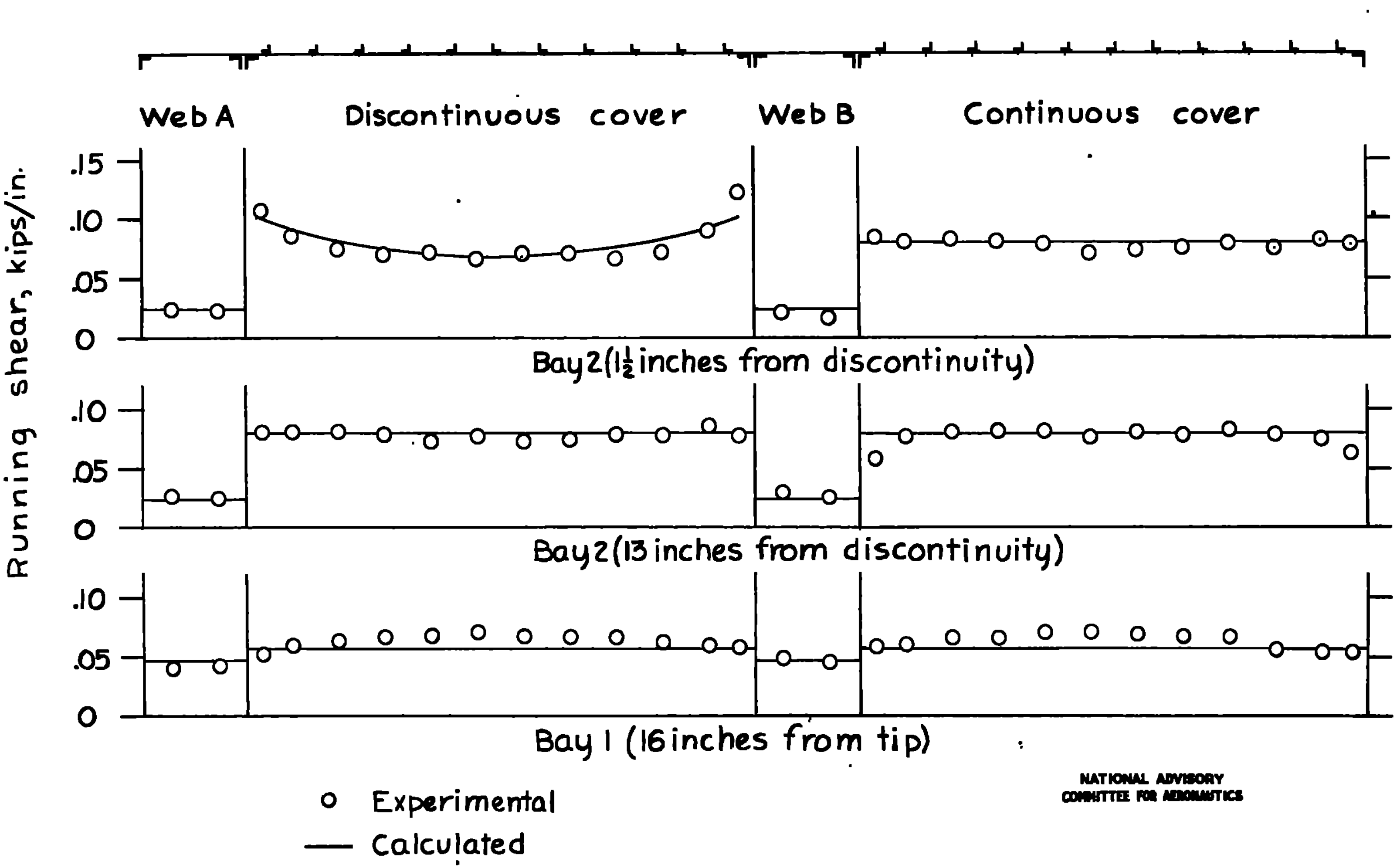

Figure 10.- Distribution of running shear along perimeter of box with stiff bulkhead at discontinuity.

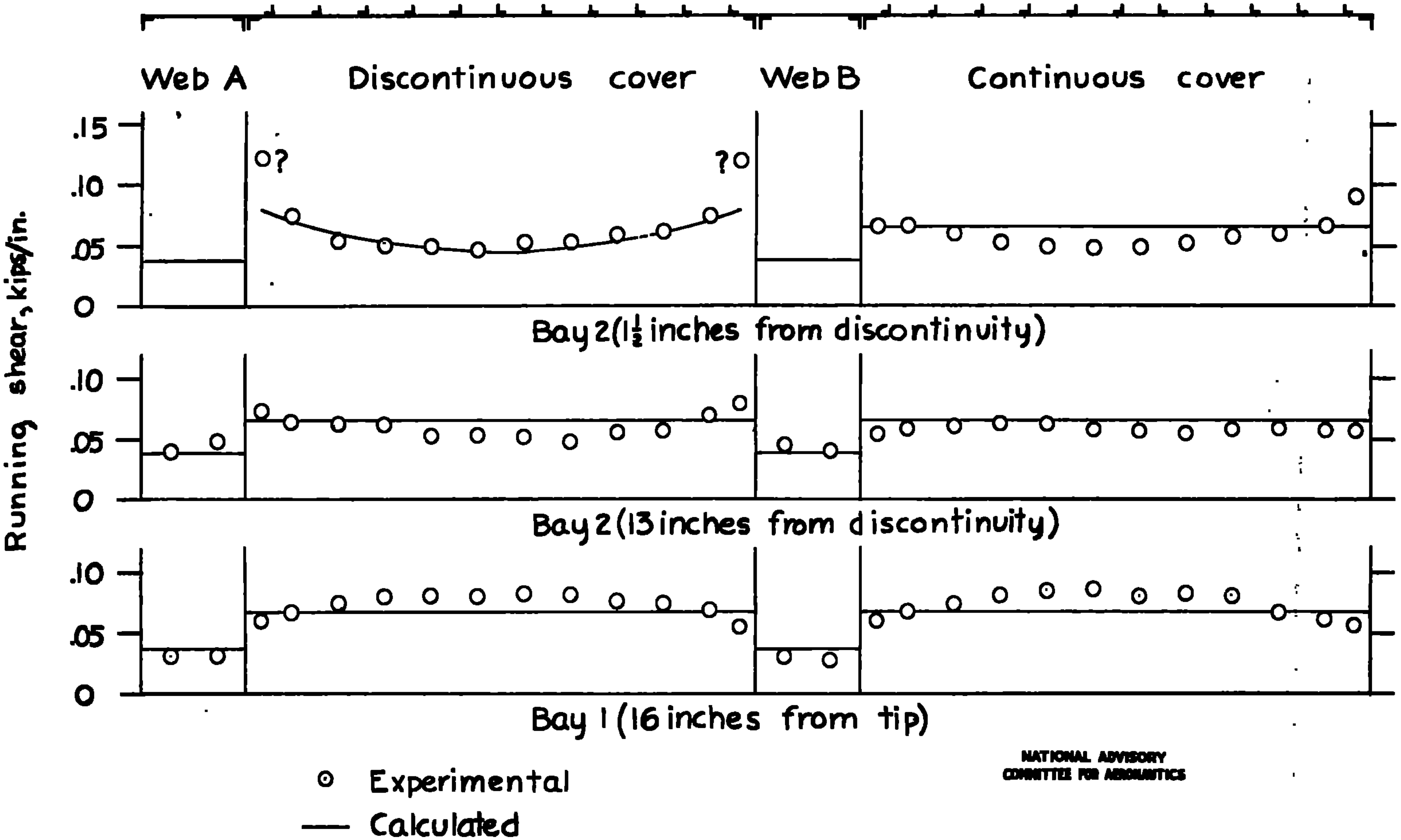

Figure 11.- Distribution of running shear along perimeter of box with flexible bulkhead and stiff cap-strip at discontinuity.

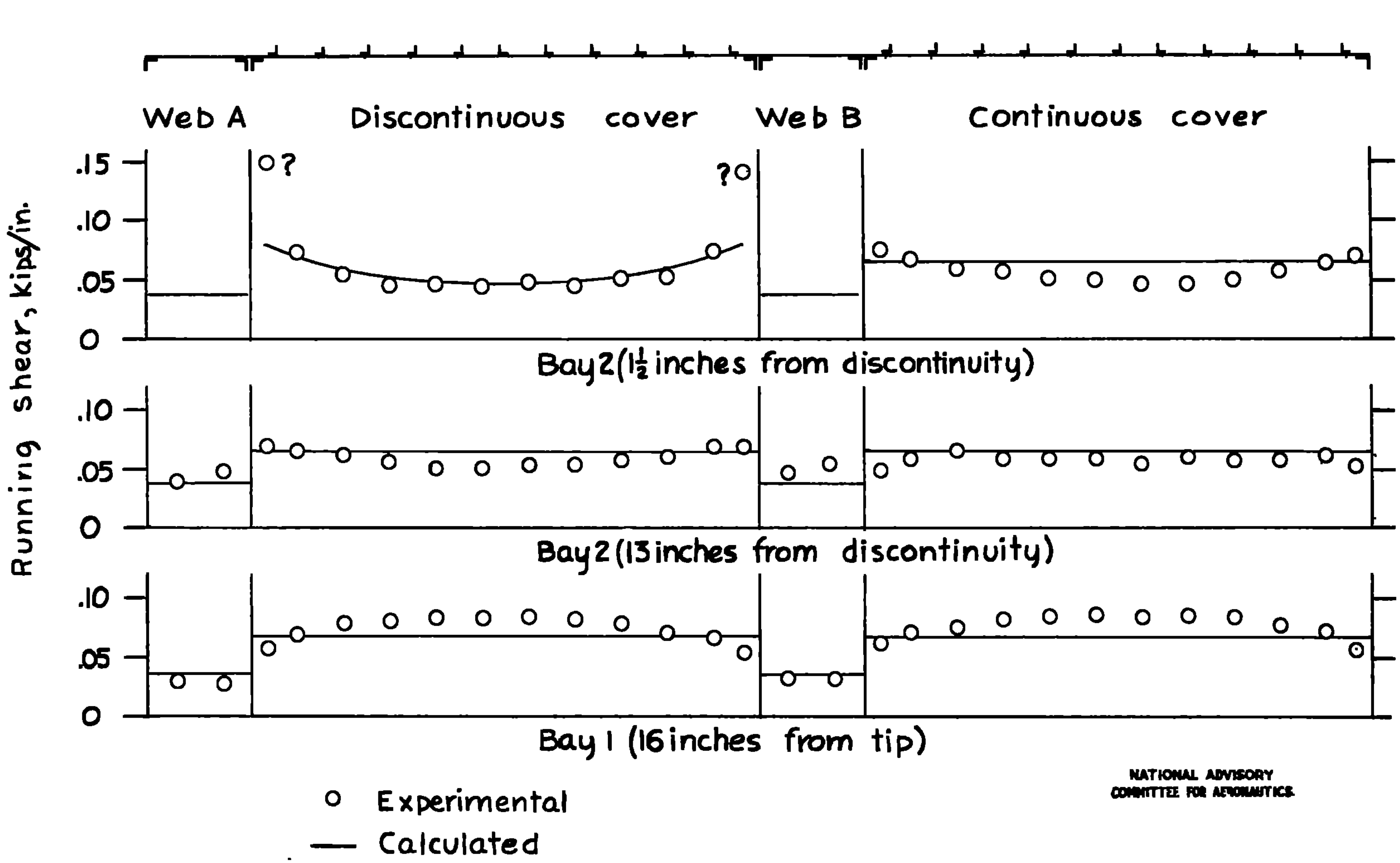

Figure 12.- Distribution of running shear along perimeter of box with flexible bulkhead and flexible cap-strip at discontinuity.

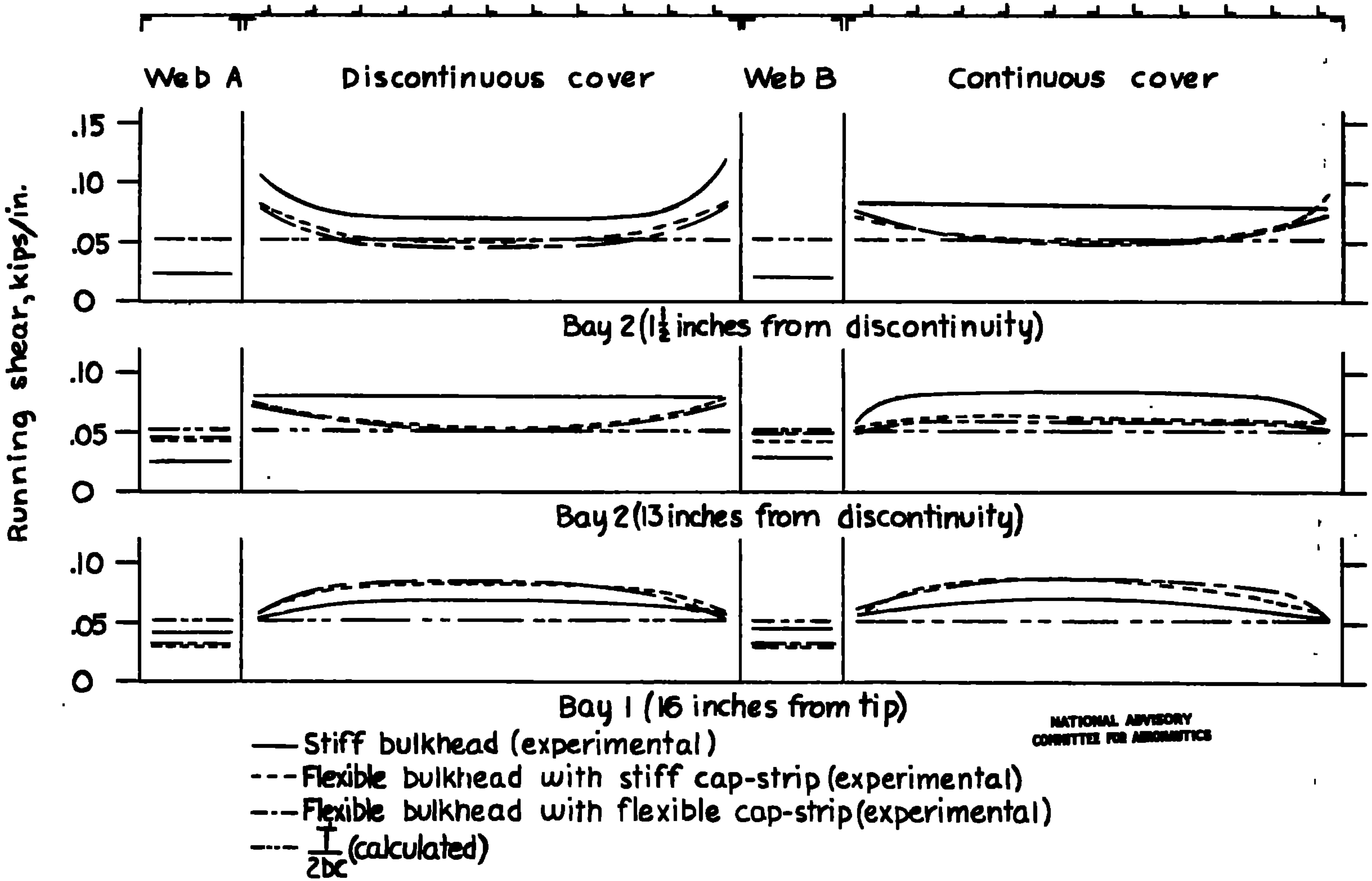

Figure 13.- Distribution of running shear along perimeter of box for the three types of bulkhead used.